

Evidence for Charging and Discharging of MoS₂ and WS₂ on Mica by Intercalating Molecularly Thin Liquid Layers

Hanlin Li, Sviatoslav Kovalchuk, Abhijeet Kumar, Dianjing Liang, Bradley D. Frank, Hu Lin, Nikolai Severin, Kirill I. Bolotin, Stefan Kirstein,* and Jürgen P. Rabe

Transition metal dichalcogenides (TMDCs) are often mechanically exfoliated on mica and examined under ambient conditions. It is known that above a certain relative humidity, a molecularly thin layer of water intercalates between the mica and the TMDC. Herein, the effect of molecularly thin liquid layers on the optical spectra of MoS₂ and WS₂ exfoliated on dry mica and exposed to the vapors of water, ethanol, and tetrahydrofuran (THF) is investigated. Photoluminescence and differential reflectance ($\Delta R/R$) spectra on the TMDCs on dry mica show dominant trion emission due to n-doping. Intercalation of water removes charge doping and results in purely neutral exciton emission, while an ethanol layer, which can be reversibly exchanged with water, does not completely suppress charge. Similarly, THF intercalates between TMDC and mica, as shown by atomic force microscopy, but it does not suppress the charging of mica. In MoS₂ bi- and trilayers, an intercalated water layer leads to a near doubling of the intensity of the indirect band transition. The described charging/discharging of TMDCs by molecular thin liquid layers can provide important clues to better control the optical properties of TMDCs under environmental conditions.

properties of the substrate and the interface between substrate and TMDC have a crucial influence on the mechanical and electronic properties of the TMDC. Three main reasons are responsible for that: first, the adhesion to the surface may induce internal strain to the TMDC, which is well known to affect the electronic band structure.^[6,7] Sometimes this strain effect is even used to tailor electronic properties.^[8–10] Strain is a particular problem when the TMDCs are mechanically exfoliated but could as well be induced by the roughness of the surface. Second, charge transfer between substrate and TMDC may happen and cause charge doping.^[11] For example, an excess of negative free charge carriers (n-doping) in TMDCs enables additional pathways for emission due to the formation of charged excitons (trions) which appears at lower energy due to higher binding energy.^[12,13] Third, the dielectric constant of the surrounding

1. Introduction


Monolayers of transition metal dichalcogenides (TMDC) possess outstanding electronic properties, which is why they are considered as promising materials for advanced applications in optoelectronics.^[1–4] These 2D materials are primarily prepared or grown on a solid substrate, besides some rare applications where TMDCs are used as free-standing membranes.^[5] The

medium has an impact on the electronic band structure and the energy levels of the excitons of the TMDC.^[14–18] The large interfacial contact area of the TMDC to the supporting substrate causes high sensitivity to all the three effects. This can be a problem, but on the other hand this sensitivity makes the monolayers promising sensors to probe the properties of the interface to the substrate. Furthermore, adsorbates of molecules on top of the TMDC also modify its electronic structure by charge-transfer processes^[19,20] which could lead to applications as gas sensors. Moreover, lateral variations of the topography and dielectric constant of the substrate might also induce local strains^[21] and local changes in the band and excitonic structure^[22] of the monolayers.

Reliable and reproducible investigations of TMDCs require well-defined, preferably atomically flat and laterally homogeneous substrates, which must be clean with respect to any molecular adsorbents. Hexagonal boron nitride meets these requirements.^[23] However, it has the disadvantage of limited availability of high-quality large-size crystals. Muscovite mica is another appealing candidate as it is a natural layered material, which can be readily cleaved, granting clean and atomically flat areas up to the order of square centimeters in size. Exfoliation of 2D materials onto a freshly cleaved mica surface under controlled environment results in well-defined interfaces of the 2D materials with the substrate.^[24] However, mica has a very high surface energy (300 mN m⁻¹, 4.2 times the value of water) which makes

H. Li, D. Liang, B. D. Frank, H. Lin, N. Severin, S. Kirstein, J. P. Rabe
Department of Physics & IRIS Adlershof
Humboldt-Universität zu Berlin
12489 Berlin, Germany
E-mail: kirstein@physik.hu-berlin.de

S. Kovalchuk, A. Kumar, K. I. Bolotin
Department of Physics
Freie Universität Berlin
14195 Berlin, Germany

 The ORCID identification number(s) for the author(s) of this article can be found under <https://doi.org/10.1002/pssa.202300302>.

© 2023 The Authors. physica status solidi (a) applications and materials science published by Wiley-VCH GmbH. This is an open access article under the terms of the Creative Commons Attribution License, which permits use, distribution and reproduction in any medium, provided the original work is properly cited.

DOI: 10.1002/pssa.202300302

the surface very hygroscopic.^[25] If it is not cleaved in ultrahigh vacuum or under dry nitrogen, the formation of a water layer on the surface of freshly cleaved mica is unavoidable.^[26,27]

When 2D materials are applied to mica, a water layer spontaneously forms between the mica and the 2D material under ambient conditions and the formation of this layer has been studied in detail using graphene as an example^[24,28–31] but also for other 2D materials, such as TMDCs.^[32–34] It was found for graphene that it becomes negatively charged (n-doped) and strained when exfoliated under dry conditions on freshly cleaved mica (where no adsorbed water layer was present). The degree of doping and strain can be unambiguously measured by Raman spectroscopy, as the two most dominant vibrations respond specifically to these two factors.^[24] The exposure of such a sample to humid air with relative humidity (RH) above a certain threshold level, typically ranging around 15–20%, leads to the intercalation of a water layer into the mica–graphene interface. Through this layer, an originally existing strain within graphene relaxes and an originally existing doping disappears.^[24] Subsequent exposure of the sample to ethanol vapor leads to exchange of the water against an ethanol layer, and vice versa.^[35,36] This exchange of the liquids affects only the doping of graphene but not the strain. On top of an ethanol layer the graphene is n-doped, comparable to the case when no liquid layer is present. The strong n-doping of graphene on top of dry mica was assumed to be due to charge transfer of electrons from trap states of mica into graphene.^[35] Reduction of doping on top of water layer is then the result of suppression of this charge transfer by a drop of surface potential due to an effective dipole layer of water. Ethanol is shown to provide a dipole layer with lower strength, which still allows charge transfers from mica, hence resulting in n-doped graphene.^[35] The release of strain in graphene on a liquid layer is attributed to the lubricating effect.^[37,38]

When monolayers of WS₂ and MoS₂ are exfoliated on dry mica and then subjected to a vapor of water or ethanol, also molecular thin layers of water or ethanol form and intercalate the interface between TMDCs and mica.^[36] The liquid layer grows at partial vapor pressures above a certain value (typically RH = 10–20% for water) and continues to fill the TMDC/mica interface completely and homogeneously within a limited time (less than 30 min). The scanning force microscopy (SFM) investigations could not provide any hints for water or ethanol molecules adsorbed on top of the TMDC, while the exchange between ethanol and water with alternating application of respective vapor was demonstrated.^[36] However, different morphologies in the wetting film were found for water and ethanol, and it was argued that they are due to an interplay of line tension and electrostatic repulsion induced by an electrostatic dipole layer resulting from the water or ethanol layer.^[36]

Besides mica, also other materials have been used as substrates for the investigation of a wetting layer, such as SiO₂^[39] or platinum.^[40] However, the water layer formation on SiO₂ needed very long time (days) under high humidity conditions^[39] and the intercalation of water between graphene grown by chemical vapor deposition (CVD-grown) and Pt(111) surface needed immersion into water at high temperature for 16 h.^[40] Other substrates, such as Al₂O₃, show too high surface roughness^[41] to observe the formation of a monolayer of a liquid with SFM. Although it would be desirable to study the effects of a water layer

on TMDCs on a variety of substrates, these examples show already that this may require conditions that are incompatible with the desire for interchange of different liquids. For this reason, we will limit ourselves to using mica as a substrate and raise the following question: If an intercalating molecularly thick water or ethanol layer is capable to induce a change of strain and doping of graphene, and the electrostatic potential of the liquid layer causes different wetting dynamics: to which extent does a liquid layer of water, ethanol, or other solvent, intercalated between mica and a TMDC, influence the mechanical and/or electronic properties of the TMDC?

This question is answered here by studying the photoluminescence (PL) and differential reflectance ($\Delta R/R$) spectra of mono-, bi-, and multilayers of WS₂ or MoS₂ that are mechanically exfoliated on dry mica and subsequently exposed to vapors of water, ethanol, and tetrahydrofuran (THF). The vapors cause a molecularly thin liquid layer to form between the mica and the TMDC, which is explicitly demonstrated here with atomic force microscopy (AFM) for the case of THF. By alternate exposure of the sample to the vapors, the liquid layers are reversibly exchanged with each other and the corresponding changes in PL spectra are tracked. The changes of the PL as a function of the liquid layer are discussed and interpreted as charging/discharging effects of the TMDC. It is assumed that the charging is due to the mica, while the liquid layers shield it by their electrostatic potential with different effectiveness. All experiments will be done at room temperature. Relevant changes in the emission spectra only are expected at low temperatures,^[42] which would require observation under vacuum. Although, for example, water films can remain stable under graphene even in ultra-high vacuum (UHV),^[43] this would make it impossible to observe the PL in situ while the liquid film is replaced. Increase in temperature mostly affects the evaporation of the liquid and might lead to inhomogeneous films.^[33]

Although we restrict to room temperature and mica as substrate, the results may provide important clues for a better understanding and control of the optical properties of TMDCs under environmental conditions.

2. Experimental Section

WS₂ and MoS₂ monolayers were mechanically exfoliated onto a freshly cleaved muscovite mica (Ratan mica, V1—optical quality) from WS₂ and MoS₂ synthetic crystals (2D semiconductors) by the tape-free mechanical exfoliation method.^[31] The samples were prepared in a glove box (LABmaster, M. Braun InertgasSysteme GmbH) filled with dry nitrogen with both oxygen and water content less than 10 ppm. For Raman investigations, mica sheets were then fixed onto a home-built steel cell with TMDC flakes facing the inner cell chamber, such that the mica sheets were working as semitransparent lids. The cell was then additionally sealed in a plastic box and transferred to a confocal microscope equipped with a spectrometer (XploRA, Horiba), or to another lab for the reflectivity measurements. The cell was then removed from its plastic box and connected to a dry nitrogen source (in case of measurements at the XploRA instrument: Linde group, 99.999% purity as specified by the manufacturer) within a few seconds for purging of the inner cell chamber. PL was acquired with a confocal Raman

microscope (XploRa, Horiba Ltd.) equipped with 600 nm^{-1} grating. Green laser light (532 nm) was used for excitation with a continuous wave (cw) illumination intensity of less than 0.01 mW through a $100\times$ objective with $\text{NA} = 0.6$, resulting in a power density of less than 1.0 kW cm^{-2} . Optical reflectivity measurements and some of the PL measurements were done in a home-built confocal PL/reflectivity setup. PL measurements were done using a 532 nm cw laser and we used an Andor spectrometer with 300 and 600 lines mm^{-1} gratings. Reflectivity measurements were carried out using a broadband pulsed super-continuum laser source (SuperK, 400–1000 nm).

For the vapor supply, a device was prepared as sketched in **Figure 1a**. Dry nitrogen is either directed purely through the cell or after bubbling through clean water or ethanol (absolute, 99.8%, ALDRICH). For water this resulted in a RH above 50%. The sample was purged with the respective gas for at least half an hour before spectral characterization, if not stated otherwise. For experiments with controlled mixing ratio between dry nitrogen and the respective vapor, a gas mixing controller GB 2000 (MCQ Instruments) was used. The mixing ratio is controlled by the respective volume flow and the numbers given in the text refer to the relative volume flow (20% ethanol means 20% volume per time bubbling through ethanol and 80% volume per time dry nitrogen). The RH was measured in a separate bottle connected to the gas mixer with a Testo 625 thermo-hygrometer (Testo Inc.) which has an accuracy of $\pm 2.5\%$. The provided values are the displayed ones. Monolayers (1L-MoS₂ or 1L-WS₂) are identified by reflection microscopy from their color contrast (**Figure 1b**) before the sample is mounted upside down in the measuring cell (**Figure 1c**). The cell fits below the objective of a confocal microscope and remains connected to the gas mixing system during the whole measurement time.

For AFM imaging, the samples were sealed in a gas-tight AFM sample cell inside the glove box, and then transferred to an AFM instrument (Cypher-ES, Asylum Research/Oxford Instruments). The cell was then purged with the dry nitrogen. The concentration of liquid vapors was controlled by mixing the dry nitrogen with nitrogen bubbling through a gas washing bottle filled with the respective liquid using the gas mixer GB 2000 (MCQ Instruments). RH was measured with a Testo 625 thermo-hygrometer. Relative vapor pressure of ethanol and THF vapors was estimated assuming saturated vapor pressures

for nitrogen bubbling through the respective liquid. We emphasize that the samples remained unexposed to ambient air before and during PL acquisition and AFM imaging.

For the gating experiments using ionic liquids, parts of the MoS₂ flakes were covered with gold by sputtering using a mask. A droplet of ionic liquid was deposited onto the flake covering also part of the gold electrode. In order to form a capacitor-like device, ionic liquid was used as a dielectric material between the gold electrode and the gate bias, formed by a PtIr wire immersed into the ionic liquid. The ionic liquid was diethylmethyl (2-methoxyethyl)ammonium bis(trifluoromethylsulfonyl)imide (commercial name of 727679 SIGMA-ALDRICH, and a purity of 98.5%). Typical gate voltages applied were in the range of $\pm 1\text{ V}$.

3. Results

In the following, we first describe the behavior of the PL and reflectivity spectra of WS₂ flakes exfoliated on mica within dry environment and after exposure to water or ethanol vapor. Furthermore, the spectral changes of the WS₂ upon exposure to THF—a nonpolar liquid—are explored. The implication of using multiple layered MoS₂ is also shown and discussed.

3.1. Water or Ethanol Intercalating between Mica and 1L-WS₂

It was demonstrated by SFM investigations^[36] that ethanol forms a homogeneous layer with a thickness of $3.5 \pm 0.3\text{ \AA}$ between the WS₂ and mica if ethanol vapor is applied with a partial pressure above $\approx 10\%$ of saturation pressure. Typically, a complete layer is formed much faster than within 30 min. Similarly, it is known from previous experiments^[24,30,35,36] that a homogeneous layer of water with a thickness of $2.8 \pm 0.3\text{ \AA}$ forms between MoS₂ (or WS₂) and mica if water vapor is applied with a RH above 15–20%. The layer forms within a time of substantially less than 30 min.^[24,30,35,36] The ethanol and water films intercalating the graphene–mica interface can be exchanged by each other exposing the samples to the respective vapors.^[36]

In **Figure 2a**, PL spectra are shown for 1L-WS₂ recorded within dry N₂ environment and after exposure to ethanol vapor and subsequently to water vapor. It is important to note that for the dry case the samples have never been exposed to humid air before

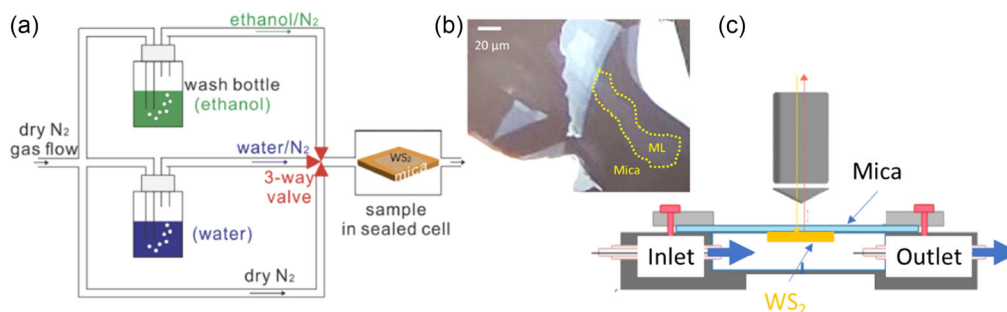


Figure 1. a) Sketch of setup to control gas mixtures within a sealed sample holder. b) Microscopic image of WS₂ flakes mechanically exfoliated on mica. The monolayers were identified by their contrast of reflected white light; one is marked by a yellow dotted line in the image. c) Schematic view of sealed sample chamber used for PL measurements. The mica is used as transparent sealing for microscopic measurements; the sample is initially prepared and inserted into the cell under dry nitrogen within a glove box (see text for detailed description).

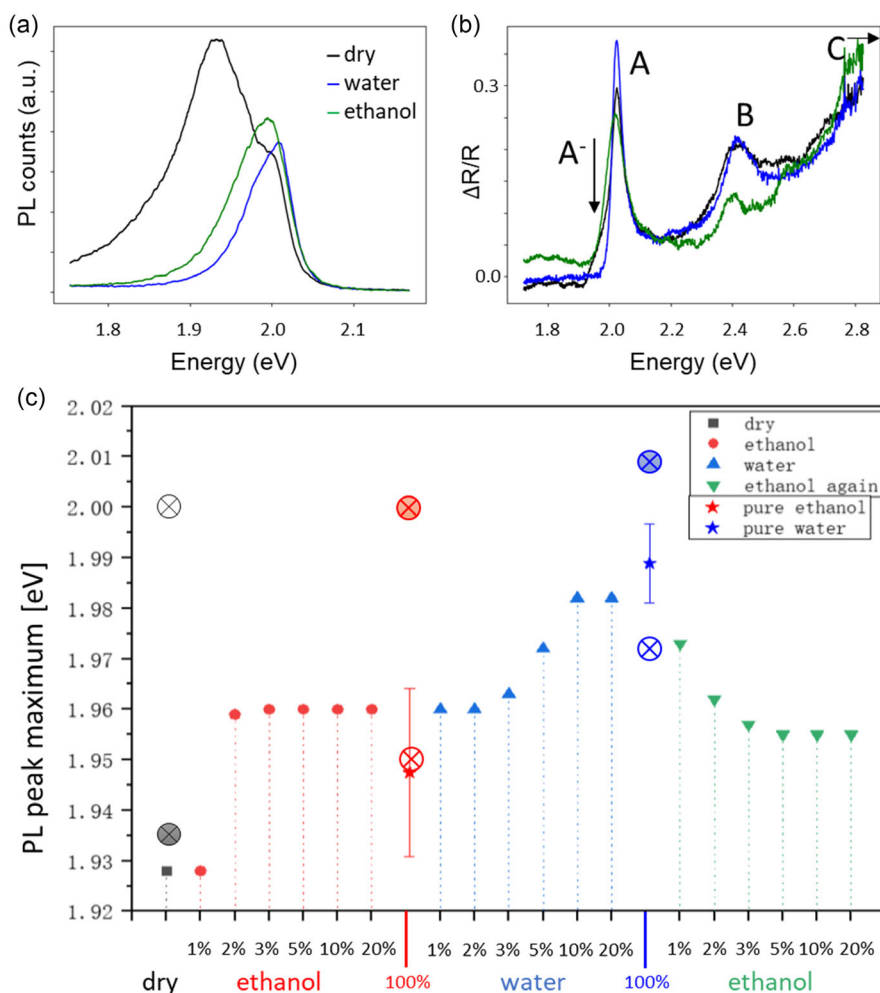


Figure 2. a) PL and b) differential reflectance spectra of WS₂ exfoliated onto mica under dry conditions (“dry,” black curve) and after exposure to water vapor (“water,” blue curve). Additionally, measurements for exposure to ethanol vapor are presented (“ethanol,” green curve). Note the very different scale of the energy axes for (a) and (b). PL excitation was at 2.33 eV with power density of 1.4 kW cm⁻². c) Dependence of PL peak maximum on the mixing rate of each vapor, recorded 10 min after change of condition. The red and blue stars indicate the peak position of samples with nitrogen bubbling through pure ethanol and pure water. The error bars indicate variations of peak position (standard deviation) between different samples. The crossed circles indicate the peak maxima of the exciton and trion peaks as obtained from fits of the spectra shown in (a). Shadowing indicates the dominant intensity.

the measurement. We therefore assume that the TMDC flakes are in direct contact to the mica surface, without a water layer in between.^[24] The ethanol or water vapor was applied for at least 30 min before measurement was started. A strong difference between PL emission of the dry sample and the one with the water layer is seen, while the emission of the sample on an ethanol layer is more like the one with water layer. The PL spectra could be well fitted by decomposition into a band from the neutral exciton (A) and a band from the charged trion (A⁻). The fits can be found in the Supporting Information and the relevant data are listed in **Table 1**. The spectrum of the sample on the water layer reflects very well the spectrum of almost unstrained and undoped WS₂^[44] which is dominated by the A emission at 2.01 eV and a small contribution of trions separated by ≈30 meV. In contrast, the emission of the sample on dry mica is dominated by trion (A⁻) emission and only a small contribution from the A emission becomes visible as a shoulder at the

Table 1. Peak positions of PL spectra of Figure 2a as obtained from fitting with a Gaussian for (A) and an asymmetric Gaussian for (A⁻). The PL peak represents the maximum as read out from the spectrum. See Supporting Information for the qualitative fits.

	Dry	Ethanol	Water
A peak [eV]	2.00	2.00	2.01
A ⁻ peak [eV]	1.935	1.950	1.972
PL peak [eV]	1.935	1.99	2.01
I(A ⁻)/I(A)	2.2	0.45	0.48

spectrum. The appearance of this shoulder is usually not observed and in this special case it may be induced by imperfect sealing of the sample leading to partial wetting of the WS₂ mica interface. The intensity ratio between trion and exciton now is just opposite to the case on water. For the sample on ethanol

layer, the spectrum is more like the case on water, but now with increased separation (by ≈ 50 meV) of the trion from the exciton. In all three cases the neutral exciton peak remains at almost identical position. For a quick analysis of the behavior of the PL emission upon changes of the liquid layers, we will refer to the PL maximum, which is simply the maximum of the whole experimental PL spectrum. These numbers are given in Table 1 as well.

The respective differential reflectivity ($\Delta R/R$) spectra of the same sample are presented in Figure 2b. They provide a good approximation for the absorption^[45] and clearly show the A and B exciton peaks of WS₂ at 2.05 and 2.45 eV, respectively. The C exciton follows at higher energies out of the measurement range. It is confirmed here what was obtained from the fits of the PL spectra: the peak position of the A exciton (and B exciton) does not appreciably change for all of the three environmental conditions. However, at the low energy edge of the A exciton band, a small shoulder becomes visible which is more prominent for the dry case and a bit less for the ethanol case (indicated by an arrow in Figure 2b). This shoulder can be assigned to trion excitation.

In summary, we state here that the PL emission of dry samples is due to charged excitons while emission with intercalated water or ethanol layer is governed by neutral exciton emission. The same behavior is observed for MoS₂, although it is not so obvious from the spectra. An example is shown in the Supporting Information.

The spectra could also be gradually shifted when mixtures of water and ethanol vapors were applied. In Figure 2c, a trace of the PL peak maximum is plotted while the ethanol or water content of the ambient vapor was gradually changed. Between each measurement, a waiting time of at least 10 min was included to equilibrate the sample. The vapor was controlled by mixing nitrogen saturated by bubbling through the respective solution with dry nitrogen (e.g., 10% ethanol means: 10% of the dry nitrogen is flowing through EtOH). At the first application of ethanol, the PL peak shifts already at very low concentrations from the position of dry samples to the ones of a complete ethanol layer. It stays constant during increase of ethanol vapor content. Obviously, a homogeneous ethanol layer formed between mica and 1L-WS₂ already with a low concentration vapor. The exchange against water took place gradually and typically was completed for a percentage of water vapor of about 20%. The exchange of water against ethanol appeared again at low concentrations of ethanol vapor; less than 3% was enough. Nevertheless, the spectral position ends up at almost the same position as for the previous ethanol layer grown on dry mica. Here, only the PL peak maximum is plotted to emphasize the behavior upon change of environmental condition. The detailed spectra are shown in the Supporting Information. The plot in Figure 2c shows not only the peak position of one selected sample but also the mean position with standard deviation for a multitude of different samples when exposed to pure water or ethanol vapor (star symbols). Although there is a strong variation in the absolute position at each condition, the difference between the respective positions varies much less and always has the same direction. For comparison, the positions of the exciton and trion peaks obtained from the fits of PL spectra shown in Figure 2a are also plotted. The A-peaks and the resulting PL maximum peaks for the ethanol and water condition are shifted toward higher energies compared to other samples. This applies specifically to this sample

and is within the generally observed flake-to-flake variation of the PL maxima. This plot emphasizes again that the spectral change from the dry case to the wet case (wet by ethanol or water) is caused by change from mainly trion to mainly exciton emission.

3.2. Intercalation of THF between Mica and WS₂

Water and ethanol are both polar liquids (polarity of 1 and 0.65 on Reichardt scale^[46]) and the molecules have comparable dipole moments. It was questionable if less polar molecules may intercalate the TMDC monolayer/mica interface and what would be then the effect on the spectral emission. We therefore used THF (polarity of 0.21 on Reichardt scale) and bubbled through dry nitrogen to obtain a vapor saturated with THF. As mica is highly hydrophilic and WS₂ is expected to be more hydrophobic, it is not obvious that a film of THF is forming a layer between mica and WS₂. Therefore, in a first step, the film formation was confirmed by SFM measurements, and the results are shown in Figure 3.

The flake was first imaged as exfoliated onto mica under dry nitrogen (see Figure 3a). The mica surface is known to be atomically flat and after fresh cleavage largely free of any adsorbed molecules. Topographies of molecules confined at the WS₂-mica interface are expected to become replicated by the flexible WS₂ flakes. Therefore, the flatness of the WS₂ flakes residing on mica indicates absence of molecules at the interface. The flake remains flat also with low vapor concentration of THF in nitrogen purging the cell. As we increased the THF vapor to a threshold value of 5%, we start to find elevated islands at the WS₂ flake edges that grow inward with time. Figure 3b shows the topography of the same flake as in Figure 3a exposed to a mixture of 95% dry nitrogen and 5% nitrogen bubbling through THF. The phase image (Figure 3b, inset) shows no discernible contrast between the growing islands and the flake, supporting the suggestion that the islands grow underneath the flakes. The height of the islands is 0.6 (± 0.2) nm, which roughly matches the size of a single THF molecule. Therefore, we attribute the islands to a layer of THF molecules intercalating the WS₂-mica interface. The layer growth propagated further for constant THF vapor concentration and finally fully filled the interface (not shown). The relatively compact wetting front and fast intercalation of the THF wetting layer can be considered as an indication—similarly to ethanol—of relatively low dipole density of the film.^[36]

As in the experiments with ethanol, the THF vapor was applied to WS₂ monolayers on mica and alternated with water vapor. Figure 4a shows PL spectra acquired from an initially dry WS₂ monolayer on mica, and then under flow of nitrogen bubbling through THF, bubbling through water, and then bubbling through THF again. The spectra are normalized with respect to the maximum intensity. In Figure 4b, the PL peak position is plotted versus concentration of THF and water vapor. The relative concentration of THF and water vapor was controlled by mixing with dry nitrogen flow, respectively. It is observed that the PL peak maximum shifts toward lower energies by a few meV, when the THF vapor content exceeds 3%. At higher values of THF concentration, the spectrum does not shift further, which implies that the THF layer formation is completed.

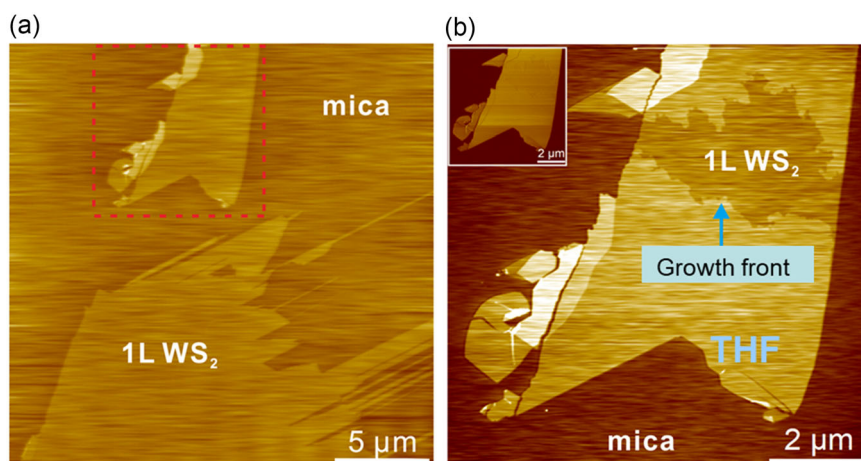


Figure 3. Topography images of a monolayer WS_2 flake on mica imaged under a) dry nitrogen and b) THF–nitrogen mixture. The front of the intercalating THF layer is labeled. The inset shows the phase image taken simultaneously with the topography image. No discernible contrast of the islands in the phase images implies them to be located under the WS_2 flake.

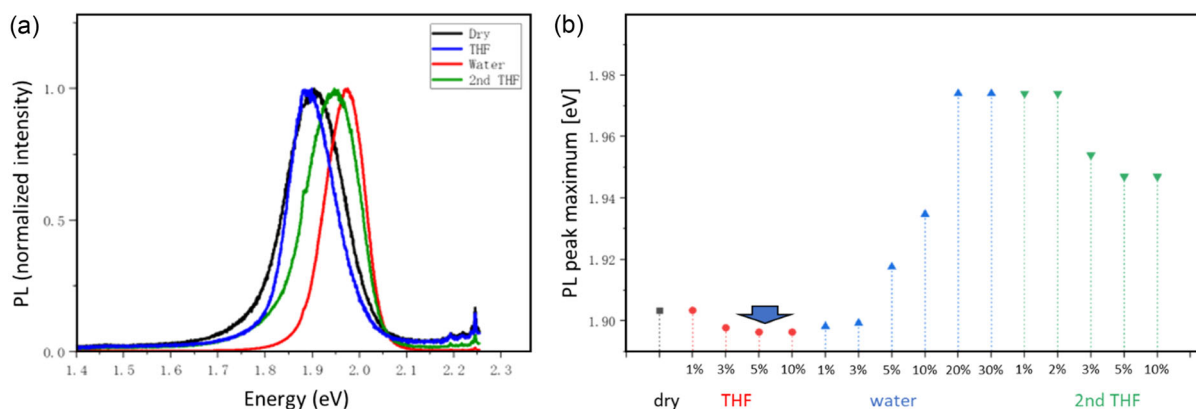


Figure 4. a) PL spectra from WS_2 monolayer on mica exposed to different vapors: dry nitrogen (black solid curve), when sample cell is filled with N_2 bubbling through THF (blue solid curve), when N_2 is bubbling through water (red solid curve), and when N_2 is bubbling through THF again (green solid curve). b) Dependence of PL peak maximum on the mixing rates of THF and water vapors. Initially, the low concentrations of THF vapor do not influence PL noticeably, then starting from 3% THF PL slightly blue shifts.

Subsequent exposure to water vapor exchanges the THF layer against a water layer, and the neutral exciton emission spectrum with a peak at 1.975 eV (in this special case) appears again. As THF is miscible with water, we cannot exclude that part of THF is remaining. On the other hand, the water layer cannot be completely removed by another subsequent exposure to THF vapor. In that case the spectrum broadens, but the maximum is not changing back to the position observed for the original THF layer. This asymmetry in exchange of liquid layers may be explained by the different wettability of mica by water and THF. The higher wettability by water due to its higher polarity favors the intercalation of water between mica and WS_2 , compared to the intercalation of THF.

3.3. Water Intercalating Mica and 2L- and 3L- MoS_2

Further insight into the mechanism that leads to the spectral shift due to the liquid layers is obtained from the behavior of double or multiple layers of MoS_2 when a liquid layer is

intercalating. In **Figure 5**, the spectra are shown collected from one flake that consisted of regions with a different number of layers. For the monolayer, the change between trion emission under dry conditions to the neutral exciton emission in humid environment was reproduced (as shown in Figure 2). For the double and triple layer, the indirect transition (I-peak) becomes visible at 1.3 and 1.4 eV, respectively. The intensities of the spectra in each plot are directly comparable because they are normalized with respect to the Raman peak of MoS_2 at 2.28 eV. The intensity of the Raman peak scales with the number of layers, which allows to identify the number of layers if the intensity for a monolayer is known. For the monolayer, the total intensity of the direct bandgap emission drops by about 30% from the neutral (A) peak in wet condition to the trion emission (A^-) in dry condition. This reduction becomes less with increasing number of layers. However, the indirect bandgap transition (I) of the double and triple layer drastically reduces in intensity by more than a factor of 2, along with a slight shift toward lower energy.

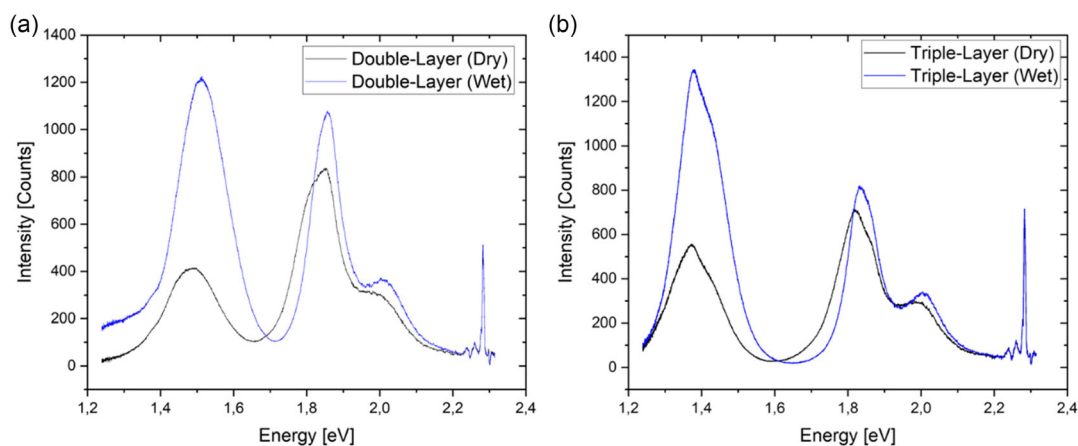


Figure 5. a) PL emission spectra of MoS₂ double layer and b) triple layer. “Dry” means prepared and kept under flow of dry nitrogen, “wet” means under flow of water vapor with RH \cong 25%. At each plot, the intensities are normalized with respect to the Raman peak of MoS₂ at 2.28 eV. Excitation energy and detector sensitivity were identical for all measurements.

The same behavior of the indirect transition is observed with electrical gating experiments using ionic liquids. In this experiment, the charging/discharging of MoS₂ was obtained by a configuration where the WS₂ acts as one electrode of a capacitor that is connected to a gold electrode and has a counter electrode via an ionic liquid. The latter is polarized by an external voltage applied via a platinum–iridium wire that is immersed into the liquid (see **Figure 6a**). Application of negative voltage of -1 V leads to discharging of the MoS₂ flake as seen in **Figure 6b** from

the emission of the A⁻ exciton, while application of positive voltages leads to charging, hence n-doping of the MoS₂. This polarity-dependent charging/discharging was verified using 1L-MoS₂ (see Supporting Information). In the discharged case, the intensity of the I-band emission is at least 2 times higher than for the charged. We conclude that the direct charging and discharging of the MoS₂ via gating causes the same spectral behavior as putting multiple-layer MoS₂ on dry or wet mica.

4. Discussion

The results show that even a molecularly thin layer of water, ethanol, or THF intercalated between mica and MoS₂ or WS₂ mono- and multilayers is capable to significantly change the emission spectra. Three different factors could be the cause of these changes: change of internal strain, change of screening by substrates with different dielectric constants, or doping by charge transfer from the surface. We want to discuss these three factors to show that doping provides the right explanation.

At first glance one might think of strain as the main reason of the observed shifts in energy of the PL intensity in analogy to graphene on mica, where strain is induced by exfoliation and the strain is released by the water layer.^[24] However, in contrast to graphene,^[38] no significant strain relaxation by lubrication could be observed for layers of MoS₂ on a water layer.^[37] However, we cannot exclude that samples are strained from the exfoliation and keep at least part of the strain during the intercalation and exchange of the liquids. This could explain the overall lowering of the exciton peaks against the unstrained value of 2.0 eV^[47] and the variation from flake to flake. A uniaxial strain of about 1% or a biaxial strain of 0.5% would be sufficient to explain these values.^[48]

However, the change of spectra, i.e., the shift of the PL peak maximum, cannot be explained by changes of strain alone. First, it would be difficult to explain the reversible switching between the spectral emission on top of water layer or ethanol layers (**Figure 2c**) by applied strain. Second, it would contradict the observation that the absorption and PL emission of the neutral A-exciton in 1L-WS₂ do not change in position or width between

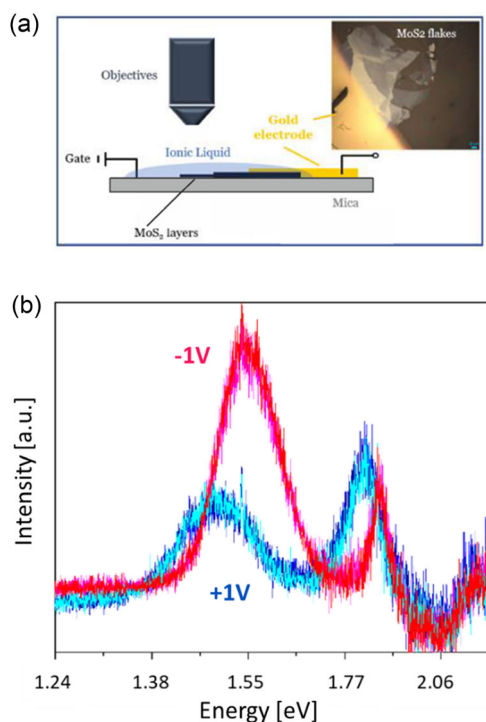


Figure 6. a) The setup used for the measurements with ionic-liquid gating. A PtIr wire immersed into ionic liquid was used as a reference electrode. b) PL spectra acquired on bilayer of MoS₂ under different gating voltages.

dry and wet conditions. From these arguments we exclude strain as the major reason for the observed changes of PL spectra, but we cannot exclude that it contributes to a certain amount.

Upon a second look one might think of changes of the dielectric constant (DC) of the underlying substrate as a major reason for the spectral changes. This could be motivated from the fact that the DCs of the three liquids are quite different. However, an increase of DC has two effects on the optical properties of TMDCs: it lowers the exciton binding energy, which results in a shift of emission toward higher energies, and additionally changes the bandgap energy.^[15,17,18] Therefore, variation of DC is expected to vary the position of the neutral exciton peak and leave the exciton/trion intensity ratio unchanged,^[15] which is in contradiction to our observation. In conclusion, we also reject DC of the liquid layers as main contribution to the observed spectral changes.

The most convincing explanation of the spectral changes is given by charge doping of the TMDCs. The change of trion position, exciton–trion separation, and exciton–trion ratio are strong indications of doping effects.^[48] That means, we assume that on dry mica (the initial state) the PL emission is almost entirely caused by trion emission. The position of this peak with respect to the neutral exciton peak is within the energy range reported in the literature for room temperature measurements on MoS₂^[49] and WS₂.^[47] What appears as a spectral shift between emission on dry substrate and on a water layer then is in fact a change of ratio between trion and exciton emission. This implies that the TMDC on dry mica must be negatively charged (n-doped) while it is discharged by the intercalating water layer. Such n-doping from mica substrate and discharging on water layer was previously found for graphene,^[24,35] where Raman emission could be employed to unambiguously determine negative charging of graphene. The charging was explained by charge transfer of electrons from trap states of mica that are present within the gap, and the suppression of doping by the electrostatic potential caused by the dipole layer of the water or ethanol molecules.^[35]

Despite the differences in the energy band structure between graphene and the TMDCs, we use similar arguments here to

describe the charging of 1L-MoS₂ and 1L-WS₂ by mica and discharging by water or ethanol. In **Figure 7**, an energy-level diagram is sketched. The diagram is based on the assumption that there are filled trap states in mica within the gap, but closer to the conduction band. The existence of such trap states was demonstrated by thermoluminescence.^[50] For a TMDC on pure mica (dry condition), these trap states are close but above the conduction band of the TMDC, which results in charge transfer of the electrons from mica to the TMDC, causing n-doping. The intercalating layer of water provides on the one hand a spacer to the TMDC but on the other hand also a step in potential energy, due to a mean orientation of the molecular dipoles.^[35] The negative sign of this potential pushes the energy level of mica downward with respect to the level of the TMDC. For water, this lowering in energy was calculated from molecular dynamics calculation to be -1.3 ± 0.1 V with respect to the level of clean dry mica.^[35] The potential values are subject to a certain degree of uncertainty, as the reference value of pure mica is not known exactly,^[35] however, this does not change the basic argumentation. At this lower position the trap states are at a level that falls in between the gap of the TMDC and hence no charge transfer is allowed. The situation is very comparable for ethanol, but with lower surface potential, which was -0.62 ± 0.11 V from molecular dynamics simulation.^[35] It is likely that in this case only few of the trap states of mica are still close to the energy of the conduction band of the TMDC. This could explain the low amount of doping of the TMDCs on ethanol. The lower doping lowers the amount of trion emission and hence the observed shift of maximum of PL emission is smaller than for the water layer. Thus, the observed “shift” of the PL maximum on ethanol and water layers is due to different ratio of neutral to charged exciton emission. In the framework of this explanation, it is clear that a non-polar liquid like THF cannot change the spectra significantly because it does not shift the energy levels and hence the charge doping.

We exclude that different distances between the TMDC and mica cause different charge transfer blocking because the THF layer has largest thickness followed by ethanol and water. Hence, if the charge transfer is controlled by distance, largest transfer would be expected for water and lowest for THF—just the opposite as observed.

A strong supporting argument for the explanation by charge transfer comes from the measurements on multilayers of MoS₂. As shown in Figure 5, the intercalating water removes emission of charged excitons at the direct bandgap emission (A), and in parallel increases drastically the intensity of the indirect band gap transition (I). The mechanism of the intensity change of the I-band is not completely understood yet. However, as PL intensity is the result of competition between radiative and non-radiative recombination channels, one may conclude that for the I-band more nonradiative recombination channels are available in the case of direct attachment of the MoS₂ onto dry mica. As also trions are created at the indirect bandgap,^[13,51,52] at the present state we only can speculate that the observed intensity change is caused by the presence of additional nonradiative recombination channels for the trions. That means, in case of charged MoS₂ on dry mica, the trions at the indirect bandgap and the non-radiative relaxation pathways from the trions cause disproportion-ate quenching of the PL intensity. The observed change of I-band

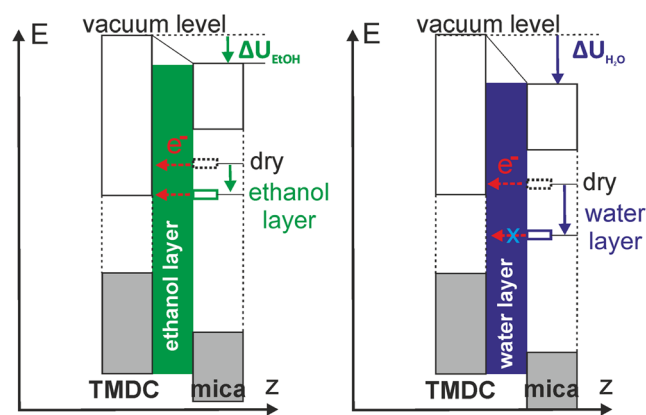


Figure 7. Sketch of energy-level alignment for the case of TMDC on mica with ethanol layer intercalating (left), and with water layer intercalating (right). The position of the trap states in mica marked by “dry” (dotted box) indicates the energy position in pure mica without water or ethanol layer on top.

intensity upon charging is in full accordance to this model of charging/discharging of MoS₂.

5. Conclusions

In conclusion, we propose that changes in optical spectra due to molecularly thin liquid layers intercalated between MoS₂ or WS₂ and mica are due to charge transfer from mica to the TMDCs. The charge transfer is blocked by polar liquids that form a dipole layer and hence a potential drop at the surface. For low polar liquids, like THF, such potential drop is missing and hence no effect on the charge transfer from the underlying mica is observed. We cannot exclude that strain also affects the spectra; however, we propose them to be of minor effect. These findings are important for all those who work with TMDCs under ambient conditions because they show that already minor changes of composition of a substrate may have huge impact on the optical properties.

Furthermore, the method demonstrated here, using polar liquid layers intercalated between a TMDC and a highly polar substrate like mica, provides an alternative approach to charge and discharge a TMDC without application of external electrodes. It opens therefore a pathway to study the optical properties on local scales on native material without further processing.

Supporting Information

Supporting Information is available from the Wiley Online Library or from the author.

Acknowledgements

This work was supported by Deutsche Forschungsgemeinschaft (Projektnummer 182087777—SFB 951) and also supported through the Cluster of Excellence “Matters of Activity. Image Space Material” under Germany’s Excellence Strategy EXC 2025, which is gratefully acknowledged (J.P.R.).

Open Access funding enabled and organized by Projekt DEAL.

Conflict of Interest

The authors declare no conflict of interest.

Data Availability Statement

The data that support the findings of this study are available from the corresponding author upon reasonable request.

Keywords

charge transfer doping, mica, photoluminescence, transition metal dicalcogenides

Received: April 17, 2023

Revised: July 20, 2023

Published online: September 22, 2023

- [1] T. Ahmed, J. Zha, K. K. H. Lin, H.-C. Kuo, C. Tan, D.-H. Lien, *Adv. Mater.* **2023**, *35*, 2208054.
- [2] J. S. Ponraj, Z.-Q. Xu, S. C. Dhanabalan, H. Mu, Y. Wang, J. Yuan, P. Li, S. Thakur, M. Ashrafi, K. McCoubrey, Y. Zhang, S. Li, H. Zhang, Q. Bao, *Nanotechnology* **2016**, *27*, 462001.
- [3] H. Lin, Z. Zhang, H. Zhang, K.-T. Lin, X. Wen, Y. Liang, Y. Fu, A. K. T. Lau, T. Ma, C.-W. Qiu, B. Jia, *Chem. Rev.* **2022**, *122*, 15204.
- [4] A. Ciarrocchi, F. Tagarelli, A. Avsar, A. Kis, *Nat. Rev. Mater.* **2022**, *7*, 449.
- [5] N. Scheuschner, O. Ochedowski, A.-M. Kaulitz, R. Gillen, M. Schleberger, J. Maultzsch, *Phys. Rev. B* **2014**, *89*, 125406.
- [6] Y. Wang, C. Cong, W. Yang, J. Shang, N. Peimyoo, Y. Chen, J. Kang, J. Wang, W. Huang, T. Yu, *Nano Res.* **2015**, *8*, 2562.
- [7] E. Blundo, M. Felici, T. Yildirim, G. Pettinari, D. Tedeschi, A. Miriametro, B. Liu, W. Ma, Y. Lu, A. Polimeni, *Phys. Rev. Res.* **2020**, *2*, 012024.
- [8] H. J. Conley, B. Wang, J. I. Ziegler, R. F. Haglun Jr., S. T. Pantelides, K. I. Bolotin, *Nano Lett.* **2013**, *13*, 3626.
- [9] Y. Qi, M. A. Sadi, D. Hu, M. Zheng, Z. Wu, Y. Jjiang, Y. P. Chen, *Adv. Mater.* **2023**, *35*, 2205714.
- [10] I. Niehues, R. Schmidt, M. Drüppel, P. Marauhn, D. Christiansen, M. Selig, G. Berghäuser, D. Wigger, R. Schneider, L. Braasch, R. Koch, A. Castellanos-Gomez, T. Kuhn, A. Knorr, E. Malic, M. Rohlfing, S. Michaelis de Vasconcellos, R. Bratschitsch, *Nano Lett.* **2018**, *18*, 1751.
- [11] J. Klein, A. Kerelsky, M. Lorke, M. Florian, F. Sigger, J. Kiemle, M. C. Reuter, T. Taniguchi, K. Watanabe, J. J. Finley, A. N. Pasupathy, A. W. Holleitner, F. M. Ross, U. Wurstbauer, *Appl. Phys. Lett.* **2019**, *115*, 261603.
- [12] K. F. Mak, K. He, C. Lee, G. H. Lee, J. Hone, T. F. Heinz, J. Shan, *Nat. Mater.* **2013**, *12*, 207.
- [13] J. Pei, J. Yang, R. Xu, Y. H. Zeng, Y. W. Myint, S. Zhang, J. C. Zheng, Q. Qin, X. Wang, W. Jjiang, *Small* **2015**, *11*, 6384.
- [14] A. Chernikov, T. C. Berkelbach, H. M. Hill, A. Rigosi, Y. Li, O. B. Aslan, D. R. Reichman, M. S. Hybertsen, T. F. Heinz, *Phys. Rev. Lett.* **2014**, *113*, 076802.
- [15] Y. Lin, X. Ling, L. Yu, S. Huang, A. L. Hsu, Y.-H. Lee, J. Kong, M. S. Dresselhaus, T. Palacios, *Nano Lett.* **2014**, *14*, 5569.
- [16] M. Florian, M. Hartmann, A. Steinhoff, J. Klein, A. W. Holleitner, J. J. Finley, T. O. Wehling, M. Kaniber, C. Gies, *Nano Lett.* **2018**, *18*, 2725.
- [17] Y. Fu, D. He, J. He, A. Bian, L. Zhang, S. Liu, Y. Wang, H. Zhao, *Adv. Mater. Interfaces* **2019**, *6*, 1901307.
- [18] A. J. Shin, A. A. Hossain, S. M. Tenney, X. Tan, L. A. Tan, J. J. Foley, T. L. Atallah, J. R. Caram, *J. Phys. Chem. Lett.* **2021**, *12*, 4958.
- [19] D. Kiriya, M. Tosun, P. Zhao, J. S. Kang, A. Javey, *J. Am. Chem. Soc.* **2014**, *136*, 7853.
- [20] M. Raoufi, S. Chandrabose, R. Wang, B. Sun, N. Zorn Morales, S. Shoaee, S. Blumstengel, N. Koch, E. List-Kratochvil, D. Neher, *J. Phys. Chem. C* **2023**, *127*, 5866.
- [21] K. P. Dhakal, S. Roy, H. Jang, X. Chen, W. S. Yun, H. Kim, J. Lee, J. Kim, J.-H. Ahn, *Chem. Mater.* **2017**, *29*, 5124.
- [22] M. Magnozzi, T. Pflug, M. Ferrera, S. Pace, L. Ramó, M. Olbrich, P. Canepa, H. Ağircan, A. Horn, S. Forti, O. Cavalleri, C. Coletti, F. Bisio, M. Canepa, *J. Phys. Chem. C* **2021**, *125*, 16059.
- [23] Y. Uchida, S. Nakandakari, K. Kawahara, S. Yamasaki, M. Mitsuhashi, H. Ago, *ACS Nano* **2018**, *12*, 6236.
- [24] H. Lin, A. Schilo, A. R. Kamoka, N. Severin, I. M. Sokolov, J. P. Rabe, *Phys. Rev. B* **2017**, *95*, 195414.
- [25] M. S. Metsik, *J. Adhes.* **1972**, *3*, 307.
- [26] S.-H. Park, G. Sposito, *Phys. Rev. Lett.* **2002**, *89*, 085501.
- [27] W. Cantrell, G. E. Ewing, *J. Phys. Chem. B* **2001**, *105*, 5434.

- [28] P. Bampoulis, K. Sotthewes, E. Dollekamp, B. Poelsema, *Surf. Sci. Rep.* **2018**, *73*, 233.
- [29] N. Severin, P. Lange, I. M. Sokolov, J. P. Rabe, *Nano Lett.* **2012**, *12*, 774.
- [30] A. Rauf, A. Schilo, N. Severin, I. M. Sokolov, J. P. Rabe, *Langmuir* **2018**, *34*, 15228.
- [31] B. Rezania, M. Dorn, N. Severin, J. P. Rabe, *J. Colloid Interface Sci.* **2013**, *407*, 500.
- [32] J. Song, Q. Li, X. Wang, J. Li, S. Zhang, J. Kjems, F. Besenbacher, M. Dong, *Nat. Commun.* **2014**, *5*, 4837.
- [33] Y. Kim, H. Kang, M. Song, H. Kwon, S. Ryu, *Int. J. Mol. Sci.* **2023**, *24*, 3492.
- [34] K. Park, H. Kang, S. Koo, D. Lee, S. Ryu, *Nat. Commun.* **2019**, *10*, 4931.
- [35] H. Lin, J. D. Cojal González, N. Severin, I. M. Sokolov, J. P. Rabe, *ACS Nano* **2020**, *14*, 11594.
- [36] A. Rauf, J. D. Cojal González, A. Balkan, N. Severin, I. M. Sokolov, J. P. Rabe, *Mol. Phys.* **2021**, *119*, 1947534.
- [37] H. Lin, A. Rauf, N. Severin, I. M. Sokolov, J. P. Rabe, *J. Colloid Interface Sci.* **2019**, *540*, 142.
- [38] H. Lin, L. Habibova, A. Rauf, J. D. Cojal González, N. Severin, S. Kirstein, I. M. Sokolov, J. P. Rabe, *Nano Lett.* **2022**, *22*, 7761.
- [39] M. J. Lee, J. S. Choi, J.-S. Kim, I.-S. Byun, D. H. Lee, S. Ryu, C. Lee, B. H. Park, *Nano Res.* **2012**, *5*, 710.
- [40] K. Verguts, K. Schouteden, C.-H. Wu, L. Peters, N. Vrancken, X. Wu, Z. Li, M. Erkens, C. Porret, C. Huyghebaert, C. Van Haesendonck, S. De Gendt, S. Brems, *ACS Appl. Mater. Interfaces* **2017**, *9*, 37484.
- [41] L. Liao, J. Bai, Y. Qu, Y. Huang, X. Duan, *Nanotechnology* **2010**, *21*, 015705.
- [42] J. Jadczyk, J. Kutrowska-Girzycka, P. Kapuściński, Y. S. Huang, A. Wójs, L. Bryja, *Nanotechnology* **2017**, *28*, 395702.
- [43] O. Ochedowski, B. K. Bussmann, M. Schleberger, *Sci. Rep.* **2014**, *4*, 6003.
- [44] M. G. Harats, J. N. Kirchhof, M. Qiao, K. Greben, K. I. Bolotin, *Nat. Photonics* **2020**, *14*, 324.
- [45] J. D. E. McIntyre, D. E. Aspnes, *Surf. Sci.* **1971**, *24*, 417.
- [46] C. Reichardt, T. Welton, in *Solvents and Solvent Effects in Organic Chemistry*, WILEY-VCH Verlag GmbH & Co. KGaA, Weinheim **2010**, pp. 549–586.
- [47] C. Cong, J. Shang, Y. Wang, T. Yu, *Adv. Opt. Mater.* **2018**, *6*, 1700767.
- [48] S. Kovalchuk, J. N. Kirchhof, K. I. Bolotin, M. G. Harats, *Isr. J. Chem.* **2022**, *62*, e202100115.
- [49] F. Cadiz, S. Tricard, M. Gay, D. Lagarde, G. Wang, C. Robert, P. Renucci, B. Urbaszek, X. Marie, *Appl. Phys. Lett.* **2016**, *108*, 251106.
- [50] N. Kristianpoller, Y. Kirsh, S. Shoval, D. Weiss, R. Chen, *Int. J. Radiat. Appl. Instrum. Part D* **1988**, *14*, 101.
- [51] S. Z. Uddin, H. Kim, M. Lorenzon, M. Yeh, D.-H. Lien, E. S. Barnard, H. Htoon, A. Weber-Bargioni, A. Javey, *ACS Nano* **2020**, *14*, 13433.
- [52] W. Zhao, R. M. Ribeiro, M. Toh, A. Carvalho, C. Kloc, A. H. Castro Neto, G. Eda, *Nano Lett.* **2013**, *13*, 5627.